Appl. Phys. B 80, 39–43 (2005)
DOI: 10.1007/s00340-004-1699-8

Applied Physics B
Lasers and Optics

J. DONG✉
J. LU
A. SHIRAKAWA
K. UEDA

# Optimization of the laser performance in $Nd^{3+}$:YAG ceramic microchip lasers

Institute for Laser Science, University of Electro-Communications,
1-5-1 Chofugaoka, Chofu, Tokyo 182-8585, Japan

**Received: 13 July 2004/Revised version: 7 October 2004**
**Published online: 23 November 2004** 

**ABSTRACT** Based on the four-level system, a theoretical model of diode-laser end-pumped fundamental continuous-wave $Nd^{3+}$:YAG ceramic microchip lasers is proposed. The fluorescence concentration quenching effect and the absorption efficiency of the host have been taken into account in the model. The theoretical results of the numerical calculations are in good agreement with those of experiments. The effects of the concentration of the $Nd^{3+}$:YAG ceramic, the thickness of the $Nd^{3+}$:YAG ceramic, and the transmission of the output coupler on the laser performance (threshold and output power) are addressed. The optimization of the concentration and the thickness for the $Nd^{3+}$:YAG ceramic microchip laser is presented. This modeling is not only applicable to the $Nd^{3+}$:YAG ceramic microchip laser but also to other four-level microchip lasers.

**PACS** 42.55.-f; 42.55.Xi; 42.70.Hj; 02.60.Cb

## 1 Introduction

Laser diode pumped solid-state microchip lasers have been attractive light sources because of their compactness, high output power, high efficiency, and so on. Owing to the short gain-medium length for microchip laser operation, the concentration of the gain medium should be high enough for absorbing enough pump power for high-efficiency operation. There are several neodymium-doped high-gain media that are suitable for microchip laser operation: $Nd^{3+}$-doped vanadate ($Nd^{3+}$:$YVO_4$), $Nd^{3+}$:YAG, etc. Although $Nd^{3+}$:$YVO_4$ crystal processes a high absorption coefficient ($31.2\,cm^{-1}$ for 1 at. % doping concentration) and a large absorption cross section ($25 \times 10^{-19}\,cm^2$) [1], it is difficult to obtain high output power operation because of its poor thermal–mechanical properties and it is difficult to grow a high-concentration single crystal. $Nd^{3+}$-doped YAG crystal has been a major laser material, but the concentration of Nd:YAG crystal grown by the traditional Czochralski method cannot be higher than 1 at. % without deteriorating the optical quality owing to the effective segregation coefficient of neodymium in YAG being only 0.2. There are some reports about the growth of highly doped Nd:YAG crystals which can be used as microchip laser gain media; however, the quality is varied along the growth axis and the highly concentrated section is in only a part of the crystal boules [1].

Recently, development of polycrystalline Nd-doped YAG ceramic laser material has attracted a lot of attention for high-power laser applications [2–8]. Compared to Nd:YAG crystal, Nd:YAG ceramic laser material has several advantages, such as easy fabrication of large-size and high-concentration Nd:YAG ceramic. It is also less expensive, may be mass produced, and so on. The laser performance of diode laser pumped Nd:YAG ceramics has been demonstrated and highly efficient operation has been achieved; a slope efficiency as high as 57.6% and an optical-to-optical efficiency of 53% have been achieved with these Nd:YAG ceramics as gain media [4]. The Nd:YAG ceramic laser material will be a promising laser material for high-power solid-state laser applications. The high concentration of Nd:YAG ceramic offers another advantage for microchip laser applications. However, there is concentration quenching with an increase of the doping concentration: the fluorescence lifetime of highly doped Nd:YAG ceramics will decrease with concentration [2, 3, 8], so the concentration effect should be taken into account when highly doped ceramics are used as microchip laser gain media. In this paper, a laser model including the concentration effect based on the rate equations is presented and analytical and numerical solutions of the laser performance (output power and pump threshold) as functions of the doping concentration and the thickness of the Nd:YAG ceramic gain medium are also presented. The numerical simulation of the laser diode pumped Nd:YAG ceramic microchip laser performance is in good agreement with the experimental results. The optimization of the doping concentration and the thickness of the gain medium as regards the laser performance is presented for guiding the design of highly efficient operation of laser diode pumped Nd:YAG ceramic microchip lasers.

## 2 Laser model

Microchip lasers are formed by directly coating dielectric films on the surfaces of a gain medium to form the laser cavities, so, in principle, they are Fabry–Pérot cavities. Alternatively, microchip lasers can be formed by directly coating a dielectric film on one surface of the gain medium

✉ Fax: +81-0424-85-8960, E-mail: dong@ils.uec.ac.jp

to form the rear mirror of the laser cavity; the output coupler is separated from the gain medium, which can be easily adjusted for optimizing other parameters to achieve optimized operation of such a laser system. The cavities can be treated as approximately concave–concave cavities with the thermal effects of the medium taken into account or plane–concave cavities. When the pump and laser beams in the gain medium are assumed to be Gaussian beams, using an $M^2$ factor, the radii of the pump and laser beams along the direction of the light can be written as [9, 10]

$$w_p^2(z) = w_{p0}^2 \left[ 1 + \frac{\left(M^2\right)^2 \lambda_p^2 (z - z_0)^2}{\pi^2 w_{p0}^4 n^2} \right] , \quad (1)$$

$$w_L^2(z) = w_{L0}^2 \left[ 1 + \frac{\lambda_L^2 (z - z_0)^2}{\pi^2 w_{L0}^4 n^2} \right] , \quad (2)$$

where $z$ is the coordinate along the axis of the laser, $w_p(z)$ and $w_L(z)$ are the radii of the pump and the laser beams at $z$, $w_{p0}$ and $w_{L0}$ are the radii of the pump and the laser beams at the waist $z = z_0$, $\lambda_p$ and $\lambda_L$ are the wavelengths of the pump and the laser, and $n$ is the refractive index of the gain medium. Generally, the length of the microchip gain medium is less than several millimeters; therefore, the approximations $w_p(z) = w_{p0}$ and $w_L(z) = w_{L0}$ may be adopted.

For a laser gain medium pumped by longitudinally continuous-wave (cw) incident pump power $P_0$, the pump rate can be written as $W_p = P_0 \eta_a / h\nu_p$, where $h$ is the Planck constant, $\nu_p$ is the frequency of the pump power, $\eta_a = 1 - \exp(-\alpha l)$ is the fraction of the incident pump power absorbed by the laser gain medium of thickness $l$, and $\alpha$ is the absorption coefficient at the pump wavelength $\lambda_p$. The normalized functions that describe the spatial distribution of the pump power and the spatial distribution of the laser cavity mode can be expressed as [11]

$$r_p(r, z) = \frac{2\alpha}{\pi w_{p0}^2 \eta_a} \exp\left( \frac{-2r^2}{w_{p0}^2} \right) \exp(-\alpha z) , \quad (3)$$

$$\varphi_L(r, z) = \frac{2}{\pi w_{L0}^2 l} \exp\left( \frac{-2r^2}{w_{L0}^2} \right) . \quad (4)$$

The total number of the laser photons in the laser cavity is defined as $\Phi = 2nlP_c / hc\nu_L$, where $P_c$ is the laser power inside the cavity, $c$ is the vacuum speed of light, $\nu_L$ is the frequency of the laser, $l$ is the length of the gain medium, and $n$ is the refractive index of the gain medium.

Because a Nd:YAG ceramic laser is a four-level system, the re-absorption of the ground state can be neglected; the rate equations including the fluorescence concentration quenching in steady state can be described as [11–13]

$$\frac{\mathrm{d}\Delta N(r, z)}{\mathrm{d}t} = W_p r_p(r, z) - \frac{\Delta N(r, z)}{\tau(N_{tot})} - \frac{c\sigma \Delta N(r, z)}{n} \Phi \varphi_L(r, z) = 0 , \quad (5)$$

where $\Delta N(r, z)$ is the spatial distribution of the population-inversion density between upper and lower laser levels in pumped conditions, $\sigma$ is the emission cross section of the gain medium at the laser wavelength, $\tau(N_{tot})$ is the lifetime of the upper-state level as a function of the concentration of the active ions, and $\tau(N_{tot})$ can be described as $\tau(N_{tot}) = \tau_0 / [1 + (C/C_0)^2]$ [3], where $\tau_0$ is the lifetime of isolated $Nd^{3+}$ ions in YAG ceramic, $C$ is the atomic percentage of the doping ions, and $C_0$ is a parameter that describes the concentration-quenching effect in Nd:YAG ceramic. The lifetime of the $^4F_{3/2}$ state of $Nd^{3+}$ ions in highly doped Nd:YAG ceramics should be governed by the sum of probabilities for several competing processes such as radiative decay, nonradiative decay by multiphonon emission, and energy transfer to other $Nd^{3+}$ ions and other impurities. The concentration-quenching effect in highly doped Nd:YAG ceramics may be ascribed to a more-short-range mechanism of the $Nd^{3+}$–$Nd^{3+}$ quenching interaction; this phenomenon plays an increasingly important role with increasing Nd-ion concentration ($Nd^{3+}$ concentration $> 1.5$ at. %). Other impurities introduced during fabrication of highly doped Nd:YAG ceramic also play an important role in the energy transfer between $Nd^{3+}$ and impurities when the Nd concentration is higher.

The corresponding equation for the total number $\Phi$ of photons in the cavity is [11, 12]

$$\frac{\mathrm{d}\Phi}{\mathrm{d}t} = \frac{c\sigma}{n} \iiint \Delta N(r, z)\, \Phi \varphi_L(r, z)\, \mathrm{d}V - \frac{\Phi}{\tau_q} = 0 , \quad (6)$$

where $\tau_q = 2nl/(c(L + T_0))$ is the cold-cavity photon lifetime, $L$ is the round-trip loss and can be expressed as $L = 2\delta l$, $\delta$ is the internal loss per unit length in the laser gain medium, $l$ is the length of the gain medium, $n$ is the refractive index of the gain medium, and $T_0$ is the output-coupler transmission.

From (5), the spatial distribution of the population-inversion density is given by

$$\Delta N(r, z) = \frac{W_p \tau(N_{tot})\, r_p(r, z)}{1 + \frac{c\tau(N_{tot})\sigma}{n} \Phi \varphi_L(r, z)} . \quad (7)$$

Substituting the population-inversion density given in (7) into (6), an implicit relationship between the pump power $P_0$ and the total laser power $P_c$ inside the cavity can be expressed as

$$4\pi l\sigma \int_0^l \int_0^\infty \frac{\tau(N_{tot}) \frac{P_0 \eta_a}{h\nu_p} r_p(r, z)}{1 + \frac{\tau(N_{tot})\sigma}{n} \frac{2nlP_c}{h\nu_L} \varphi_L(r, z)} \varphi_L(r, z)\, r \mathrm{d}r \mathrm{d}z = L + T_0 . \quad (8)$$

When the spatial distributions of the pump power and the laser power inside the cavity, (3) and (4), are substituted into (8), (8) can be rewritten as

$$\frac{8\sigma}{w_{L0}^2} \int_0^l \int_0^\infty \frac{\tau(N_{tot}) \frac{2\alpha P_0}{h\nu_p \pi w_{p0}^2} \exp\left( \frac{-2r^2}{w_{p0}^2} \right) \exp(\alpha z)}{1 + \frac{4P_c \tau(N_{tot})\sigma}{h\nu_L \pi w_{L0}^2} \exp\left( \frac{-2r^2}{w_{L0}^2} \right)} \times \exp\left( \frac{-2r^2}{w_{L0}^2} \right) r \mathrm{d}r \mathrm{d}z = L + T_0 . \quad (9)$$

Equation (9) can be simplified by integrating over the length of the gain medium; then

$$\frac{8\sigma}{w_{L0}^2}\int_0^\infty \frac{\tau\left(N_{tot}\right)\frac{2P_0}{h\nu_p\pi w_{p0}^2}\exp\left(\frac{-2r^2}{w_{p0}^2}\right)\eta_a}{1+\frac{4P_c\tau(N_{tot})\sigma}{h\nu_L\pi w_{L0}^2}\exp\left(\frac{-2r^2}{w_{L0}^2}\right)} \times\exp\left(\frac{-2r^2}{w_{L0}^2}\right)r\mathrm{d}r = L+T_0\,. \quad (10)$$

Let $x=2r^2/w_{L0}^2$, $a=w_{L0}^2/w_{p0}^2$, and $y=\exp(-x)$; then (10) becomes

$$2\sigma\int_0^1 \frac{\tau\left(N_{tot}\right)\frac{2P_0\eta_a}{h\nu_p\pi w_{p0}^2}y^a}{1+\frac{4P_c\tau(N_{tot})\sigma}{h\nu_L\pi w_{L0}^2}y}\mathrm{d}y = L+T_0\,. \quad (11)$$

In (11), if $P_c=0$, the corresponding $P_0$ is the pump threshold $P_{th}$:

$$P_{th}=\frac{L+T_0}{\int_0^1\tau(N_{tot})\frac{4\eta_a\sigma}{h\nu_p\pi w_{p0}^2}y^a\mathrm{d}y}=\frac{h\nu_p\pi w_{p0}^2\,(a+1)\,(L+T_0)}{4\eta_a\tau(N_{tot})\sigma}\,. \quad (12)$$

## 3 Numerical simulation and predictions

The laser model proposed above was used to calculate the laser performance of diode laser pumped $Nd^{3+}$:YAG ceramic lasers [4]. The parameters of the laser cavity and the Nd:YAG ceramic laser material are listed in Table 1. The experimental and calculated results of the diode laser pumped $Nd^{3+}$:YAG ceramic microchip laser are listed in Table 2; the experimental data are quoted from [4]. In this table, $P_{abs}=P_0\eta_a$, $P_{out}=P_cT_0$, and $\eta$ represent the absorbed pump power, the output power, and the slope efficiency, respectively. From Table 2, we can see that the numerical simulation of the diode laser pumped 2 at. % $Nd^{3+}$:YAG ceramic laser is in good agreement with the experiments. The numerical simulation of the output power as a function of the incident pump power for a diode laser pumped 2 at. % Nd:YAG ceramic microchip laser with 2.5-mm gain-medium length and 0.03 output-coupler transmission is shown in Fig. 1. The differences between the calculated and the experimental results shown in Table 2 and Fig. 1 may be caused by the following factors which were not taken into consideration in the laser model: the optical inhomogeneity of the ceramic gain medium, the distribution variation of the absorbed pump power along the pump direction inside the gain medium according to the Lambert–Beer law, the other losses of the laser cavity, etc. The thermal effect introduced by the absorbed pump power inside the gain medium enhances the vibration of the nanocrystalline lattice and it will reduce the quantum efficiency of the luminescence and increase the line width of the luminescence spectrum, which will increase the pump power threshold and decrease the efficiency of the laser performance. For the end-pumped microchip lasers, the absorbed pump power inside the gain medium is not uniformly distributed and decreases from the entrance of the pump power to the exit of the pump power, so a deformation inside the gain medium will be induced, which will result in more interaction between the active ions and the impurities; therefore, the loss of the ceramic will increase. In most cases, the radius of the pump power adopted in the numerical calculations is not exactly the same as that in the laser experiments because there is a measurement error when the radius of the pump power was measured. Therefore, there will be some discrepancy between the calculated results and the experimental results.

From (11) and (12), we can see that the transmission of the output coupler has an effect on the pump power threshold and the output power of diode laser pumped Nd:YAG ceramic lasers. The pump power threshold is proportional to the transmission of the output coupler, and there should

| Parameters | Value | Reference |
|---|---|---|
| $\sigma$ | $4.9\times10^{-19}$ cm$^2$ | [14] |
| $\lambda_p$ | 808 nm | |
| $\lambda$ | 1064 nm | |
| $w_{p0}$ | 70 µm | |
| $w_{L0}$ | 142.5 µm | |
| $P_0$ | 1 W | |
| $T_0$ | 0.03 | |
| $\delta$ | 0.002 cm$^{-1}$ | [8] |
| $l$ | 2.5 mm | |
| $C_0$ | 2.98 at. % | |
| $\tau_0$ | 266 µs | |

**TABLE 1** Values of the parameters used in the numerical simulation for Nd:YAG ceramic microchip lasers

| | Absorbed power (mW) | Output power (mW) | Threshold (mW) | Slope efficiency (%) |
|---|---|---|---|---|
| Experimental | 842 | 465 | 27 | 57.6 |
| Calculated | 842 | 484 | 22 | 58.6 |

**TABLE 2** Comparison of calculated and experimental results for the Nd:YAG ceramic microchip laser

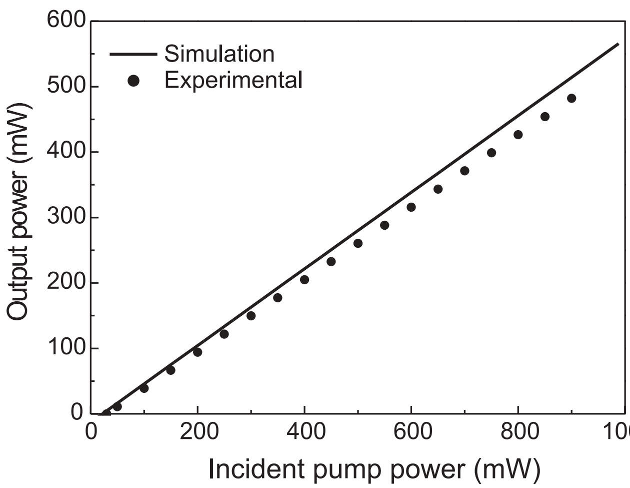


**FIGURE 1** Output power of 2 at. % Nd:YAG ceramic microchip laser as a function of incident pump power. The length of the Nd:YAG ceramic is 2.5 mm, the output-coupler transmission is 3%

be an optimizing transmission for the highest output power under a certain pump power. Figure 2 shows the pump power threshold and the output power of 2 at. % Nd:YAG ceramic with 2.5-mm thickness under 1-W pump power as a function of the transmission of the output coupler. The pump power threshold increases with the transmission of the output coupler, there is an optimal transmission of the output coupler for achieving the highest output power, and the optimal transmission for this configuration is about 0.13, the pump power threshold being 81 mW. The highest output power is about 668 mW; the corresponding optical-to-optical efficiency is 67%.

The laser performance of Nd:YAG ceramic microchip lasers strongly depends on the doping concentration of $Nd^{3+}$ ions and the thickness of the laser medium. Figure 3a shows the contour plots of the pump power threshold as a function of the doping concentration and the thickness of the $Nd^{3+}$:YAG ceramic; the internal loss per unit gain-medium length is adopted to be 0.002 $cm^{-1}$ as mentioned in [8] and the transmission of the output coupler is set to 0.03. The threshold decreases dramatically with the increase of the length of the gain medium when the gain-medium length is shorter than 0.15 mm as shown in Fig. 3b; the lowest pump power threshold is achieved when the concentration is lower than 5 at. % and the ceramic length is longer than 0.3 mm. The pump power threshold increases with the doping concentration of the gain medium when the length of the gain medium is greater than 0.15 mm because the lifetime is shortened with an increase of the doping concentration for Nd:YAG ceramic. The contour plots of the output power of an $Nd^{3+}$:YAG ceramic laser as a function of the doping concentration and the thickness of the gain medium are shown in Fig. 4a. The output power of an $Nd^{3+}$:YAG ceramic laser can be achieved by using different combinations of the doping concentration and the thickness of the gain medium. There is an area for optimizing operation of the laser; this area is within the doping concentration around 2–10 at. % and the thickness around 0.3–2 mm. The maximum output power of about 700 mW can be achieved with 1-W pump power. The output power increases dramatically with the thickness of the Nd:YAG ceramic for different concentrations of $Nd^{3+}$ ions when the thickness of the gain medium is less than 0.3 mm, as shown in Fig. 4b. This is caused by the lower absorption efficiency when the gain medium is shorter than 0.3 mm, as shown in Fig. 5. Figure 5 shows the absorption efficiency of the Nd:YAG ceramic as a function of the doping concentration and the thickness of the Nd:YAG ceramic. For the efficient operation of Nd:YAG ceramic microchip lasers, the absorption efficiency should be over 90%; there is a range of doping concentration and length product to satisfy such a requirement, as shown in Fig. 5. In this range, better laser performance can be achieved as shown in Fig. 4; the high output power and high-efficiency operation of an Nd:YAG ceramic microchip laser can be achieved.

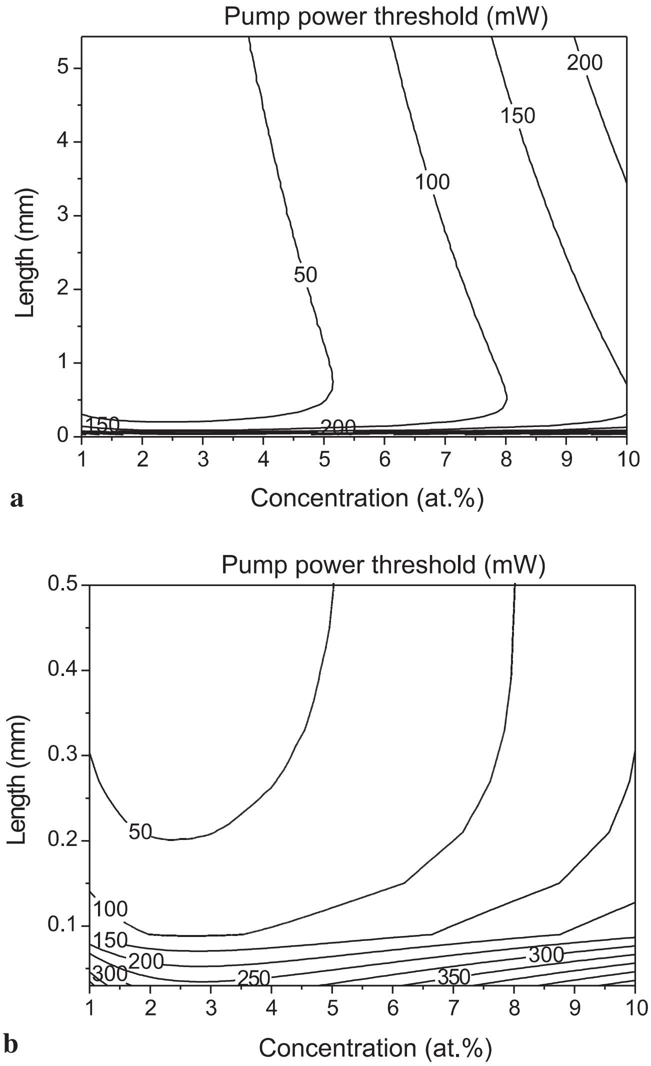


**FIGURE 3** (**a**) A family of curves for the pump power threshold of the Nd:YAG ceramic lasers as functions of the doping concentration and the thickness of the gain medium. (**b**) More detailed contour plots of the pump power threshold when the length is shorter than 0.5 mm. The transmission of the output coupler was set to 0.03

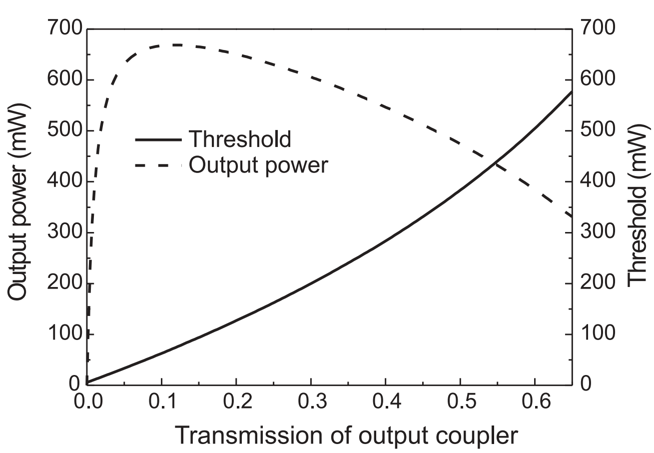


**FIGURE 2** The threshold and output power as a function of reflectivity of the output coupler. The incident pump power was set to 1 W

The value of the contour plots displayed in Figs. 3 and 4 is that parameter spaces appropriate for various possible pump power thresholds and output powers are immediately identifiable. This result implies that the laser performance of $Nd^{3+}$:YAG ceramic microchip lasers strongly depends on the doping concentration of the active ions, and it also shows that

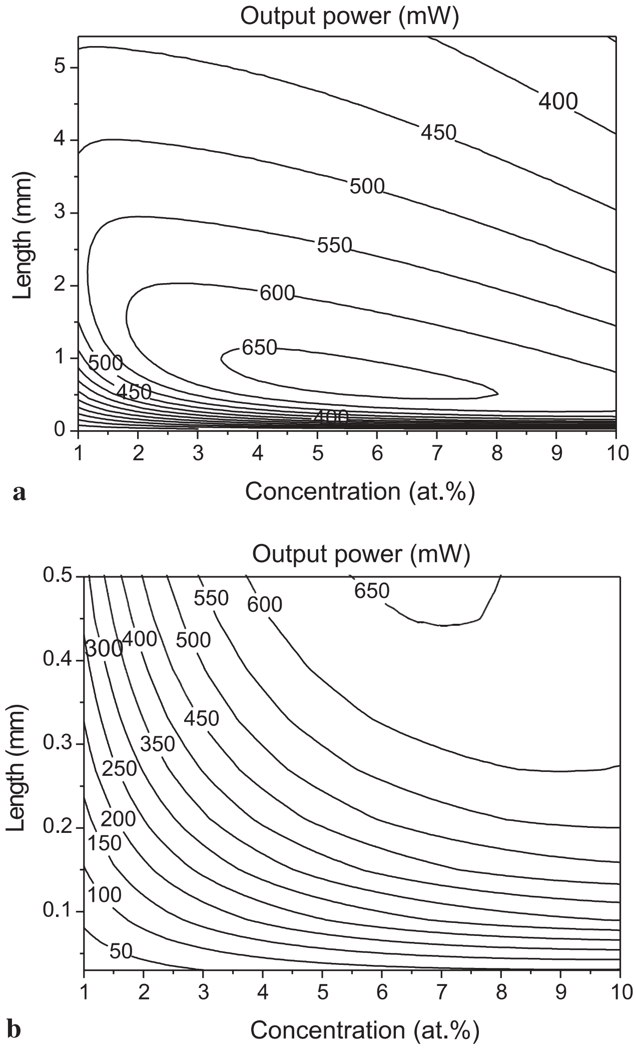


**FIGURE 4** (**a**) A family of contour plots for the output power of the Nd:YAG ceramic lasers as functions of the doping concentration and the thickness of the gain medium. (**b**) Detailed contour plots of the output power when the length is shorter than 0.5 mm. The transmission of the output coupler was set to 0.03

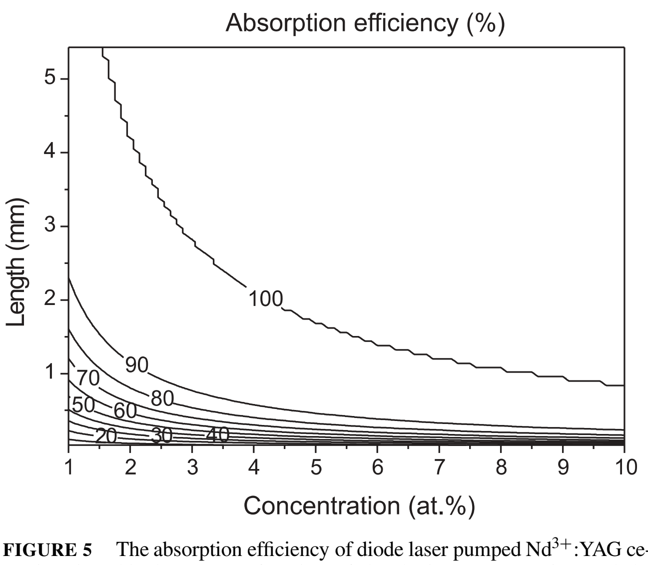


**FIGURE 5** The absorption efficiency of diode laser pumped $Nd^{3+}$:YAG ceramic microchip lasers as a function of the doping concentration and the thickness of the $Nd^{3+}$:YAG ceramic

the cause of the concentration-quenching effect must be taken into account for microchip lasers.

## 4 Conclusions

A theoretical model for cw $Nd^{3+}$-doped YAG ceramic microchip lasers including the concentration-quenching effect is proposed based on the four-level system. Other factors related to the output power of diode laser pumped Nd:YAG ceramic microchip lasers, such as the gain-medium's thickness, the doping concentration of $Nd^{3+}$ ions, the incident pump power, the transmission of the output coupler, and the fluorescence lifetime of the upper level, are taken into account. The numerical simulation of the diode laser pumped Nd:YAG ceramic microchip laser is in good agreement with experiments. From the calculation of the pump power threshold and the output power as functions of the thickness and the concentration of the gain medium, the optimized relationship between the doping concentration and the thickness of the Nd:YAG ceramic enables the microchip lasers to have a relatively low pump power threshold and a highly efficient laser operation at a certain pump power level. The effect of a decrease of the thickness will benefit the thermal management for laser operation with high-concentration Nd:YAG ceramic as gain medium. The same output power can be achieved by using a different-concentration gain medium with the relevant thickness. The optimized concentration for microchip laser operation should be over 2 at. %, and the optimized length of the Nd:YAG ceramic microchip laser should be in the range between 0.3 mm and 2 mm. This model can be also applied to other four-level cw microchip lasers.

**ACKNOWLEDGEMENTS** This work was supported by the 21st Century Center of Excellence (COE) program of the Ministry of Education, Science and Culture of Japan.

## REFERENCES

1 J. Dong, P. Deng, F. Gan, Y. Urata, R. Hua, S. Wada, H. Tashiro: Opt. Commun. **197**, 413 (2001)
2 J. Lu, M. Prabhu, J. Song, C. Li, J. Xu, K. Ueda, A.A. Kaminskii, H. Yagi, T. Yanagitani: Appl. Phys. B **71**, 469 (2000)
3 I. Shoji, S. Kurimura, Y. Sato, T. Taira, A. Ikesue, K. Yoshida: Appl. Phys. Lett. **77**, 939 (2000)
4 J. Lu, M. Prabhu, J. Xu, K. Ueda, H. Yagi, T. Yanagitani, A.A. Kaminskii: Appl. Phys. Lett. **77**, 3707 (2000)
5 J. Lu, J. Song, M. Prabhu, J. Xu, K. Ueda, H. Yagi, T. Yanagitani, A. Kudryashov: Jpn. J. Appl. Phys. **39**, L1048 (2000)
6 J. Lu, M. Prabhu, J. Song, C. Li, J. Xu, K. Ueda, H. Yagi, T. Yanagitani, A.A. Kaminskii: Jpn. J. Appl. Phys. **40**, L552 (2001)
7 J. Lu, T. Murai, K. Takaichi, U. Uematsu, K. Misawa, M. Prabhu, J. Xu, K. Ueda, H. Yagi, Y. Yanagitani, A.A. Kaminskii, A. Kudryashov: Appl. Phys. Lett. **78**, 3586 (2001)
8 J. Lu, K. Ueda, H. Yagi, T. Yanagimi, Y. Akiyama, A.A. Kaminskii: J. Alloys Compd. **341**, 220 (2002)
9 W. Kochner: *Solid State Laser Engineering*, 5th edn. (Springer, Berlin 1999) Chap. 5
10 T. Taira, J. Saikawa, T. Kobayashi, R.L. Byer: IEEE J. Sel. Top. Quantum Electron. **3**, 100 (1997)
11 W.P. Risk: J. Opt. Soc. Am. B **5**, 1412 (1988)
12 T.Y. Fan, R.L. Byer: IEEE J. Quantum Electron. **QE-23**, 605 (1987)
13 T.Y. Fan, R.L. Byer: IEEE J. Quantum Electron. **QE-24**, 895 (1988)
14 M. Sekita, H. Haneda, T. Yanagitani, S. Shirasaki: J. Appl. Phys. **67**, 453 (1990)